Upsilon Polarization and Event Activity

Brandon McKinzie*

Advisors: Manuel Calderón de la Barca Sánchez, Daniel Cebra

Abstract

This paper consists of research from two projects both focused on the Upsilon meson. For the first project, an estimate for the systematic uncertainty associated with the polarization of the Upsilon meson is presented for the LHC heavy-ion collision energy of $\sqrt{s_{NN}}$ = 2.76 TeV. Kinematic cuts are applied to simulated data in order to model the acceptance of the CMS detector. We find that Upsilon acceptance varies as a function of p_T, with, when no kinematic cuts are applied, as high as a twelve-percent difference (at low p_T) and, when kinematic cuts are applied, as high as a four-percent difference (at mid p_T). For the second project, Upsilon yields are extracted from STAR data containing $\Upsilon(nS)$ candidates produced in p-p collisions at $\sqrt{s_{NN}}$ = 200 GeV. The event-normalized $\Upsilon(nS)$ cross-sections are plotted as a function of charged-particle multiplicity and then compared to recent findings from the CMS collaboration, wherein a highly positive correlation was found between these two variables. For the case at STAR, however, the correlation is less pronounced, possibly due to a lack of event statistics.

1. Introduction

The Upsilon meson (Υ) is important for studying temperature and deconfinement in the Quark-Gluon Plasma(QGP). In such a state, the strong-force potential responsible for quark-antiquark confinement is expected to be screened by partons in the surrounding medium[1]. As a consequence, the $\Upsilon(nS)$[1] energy states are expected to sequentially melt, meaning the higher energy states will be more suppressed than the lower energy states. Such suppression has been observed at both CMS[2] and at STAR[3]. The dissociation of each Υ(nS) bound state depends on the temperature, so studying the level of this dissociation in heavy-ion collisions, when compared to p-p collisions, provides an indirect temperature measurement of the QGP. In addition, the large mass of the Υ allows for stronger theoretical predictions regarding its properties when compared to more relativistic quarkonia like the J/Ψ meson. [4]. Therefore, analyzing the Upsilon at varying energy levels and with different colliding species is a powerful probe for revealing the properties of the QGP.

In order to accurately infer characteristics of the QGP, one must have a thorough understanding of the properties of the Upsilon itself. A current unknown property of the Υ is the angle at which its daughter particles, typically two back-to-back leptons, are emitted as viewed from the Υ rest frame[4]. This frame of reference is referred to as the Center-of-Mass(CM) Helicity Frame, also known as the Recoil Frame[5]. Letting the Υ momentum lie along the x-axis, the following proportionality between the number of dileptons produced at a given polarization angle (with respect to the momentum x-axis) and the degree of polarization is found to be [2]

$$\frac{dN}{dcos(\theta^*)} \propto 1 + \alpha cos^2(\theta^*) \tag{1}$$

where α is the chosen polarization parameter, defined as

$$\alpha = \frac{\sigma_T - 2\sigma_L}{\sigma_T + 2\sigma_L} \tag{2}$$

*Funded by NSF grant PHY-1263201

[1] where n may equal 1, 2, or 3. $\Upsilon(1S)$ is the ground state and larger n corresponds to higher energy states. (This is analogous to electron energy levels in the hydrogen atom, for example.)

[2] A more in-depth treatment of polarization parameters may be found in Ref.[4]

relating the transverse and longitudinal components of the polarization production cross sections. It should be emphasized that full transverse polarization ($\alpha = 1$) would be physically realized as a preferential decay of the Υ to a lepton pair with the leptons' momenta being parallel/antiparallel to the Υ direction of momentum. Conversely, fully longitudinal polarization ($\alpha = -1$) is associated with lepton-pair production perpendicular to the Υ momentum.

Results from the D∅ and CDF Collaborations at Fermilab disagree with regard to measured levels of polarization[6][7]. Furthermore, calculations from non-relativistic Quantum Chromodynamics (nrQCD) predict strong transverse polarizations for high Υ p_T [8], which neither D∅ nor CDF observed. The current indecisive state of polarization measurements calls for an estimate of the systematic uncertainty associated with varying degrees of Υ polarization. While such estimates have been made for the STAR detector [5], the same cannot be said for the CMS detector. One of the primary aims of this paper is to provide this systematic uncertainty in order to explore possible relationships between the polarization, detector acceptance, and Υ p_T.[3]

Another interesting observation has recently been found by CMS regarding the event-normalized production cross sections of the Υ as a function of two measures of event activity, charged-particle multiplicity and transverse energy.[9]. More importantly, the charged-particle tracks are detected in the region $|\eta| < 2.4$, the same kinematic region as the observed Upsilon. Conversely, the transverse energy measurements are made in the forward region $4.0 < |\eta| < 5.2$, far from the Upsilon's kinematic region and thus less likely to be correlated with Upsilon production. As shown in Figure 1, p-p collisions seem to produce relatively more Upsilons than expected[4] when measured as a function of the aforementioned central-region charged-particle multiplicity. This region is expected to have particles more directly correlated with Upsilon production, as illustrated by the sharp increase for the p-p case. However, the positive correlation from pPb and PbPb collisions appears to be linear with a slope of unity, as opposed to the nearly parabolic correlation suggested by the p-p data.

When the Υ production cross sections are measured as a function of transverse energy deposition in the forward region, $4.0 < |\eta| < 5.2$, the correlation is linear with a slope of unity for all three collision scenarios. The difference between the two plots suggests event activity in the central region has a more positive, and perhaps more direct, correlation with Υ production than event activity in the forward region. A possi-

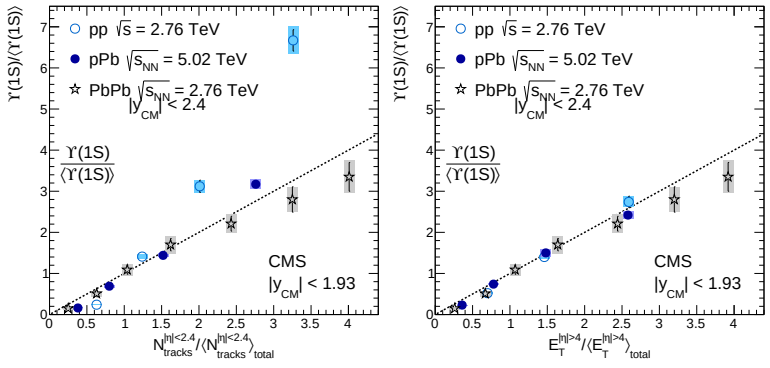

Figure 1: Data from CMS published April 28, 2014. Both Y-axes are event-normalized $\Upsilon(nS)$ yields, where the normalization is simply the average event yield from the full dataset. The X-axes are (left) the event-normalized number of tracks found in the central region $|\eta| < 2.4$ and (right) the event-normalized values of transverse energy deposited in the HF calorimeter. Data is overlaid from proton-proton, proton-lead, and lead-lead collisions.

[3]This will be the first of two projects discussed, and sections 2 - 4 will contain further information pertaining to this project.

[4]"Expected" here just means along the dotted line. The line is simply shown for illustrative purposes and does not originate from any model calculations.

ble interpretation for this is the occurence of multiple parton-parton interactions in a given p-p collision [10].

Interestingly, the cross sections for multi-partion interactions are expected to increase with increasing energy [11]. If so, it would be of value to study Υ yields against event activity in detectors designed for different energies than CMS, such as the STAR detector at RHIC. Here I attempt to replicate the CMS results below using data collected in pp-collisions at STAR in the year 2012. A similar positive correlation is found between event-normalized Υ yields and charged-particle multiplicity, although with not nearly enough statistics to make the same conclusions suggested by the CMS data.

2. Detectors and Event Selection

Both the polarization and event activity analyses assume knowledge of certain methods of detection incorporated at particle accelerators. To familiarize the reader with such methods, a brief overview of the two relevant detectors will be presented.

2.1 Compact Muon Solenoid (CMS)

One of the primary motivations for building the CMS detector was to identify muons emitted by particles in a collision[12]. This characteristic allows for the analysis of the Upsilon via a decay into a lepton pair, such as a dimuon. Muons are first identified by whether or not they make it to the muon detectors after passing through the electromagnetic and hadronic calorimeters which stop virtually all other particles. Then properties of the muons, such as momenta, may be reconstructed by measuring how much they bend in the presence of the 4-T superconducting magnet's field. The primary method of Υ identification, then, is through analysis of kinematic properties of muon pairs recorded by the muon system in order to reconstruct the Υ decay vertex.

CMS also covers a massive solid angle with respect to the collision vertex. Muon tracks may be identified in the pseudorapidity region $\mid \eta \mid < 2.4$, which allows for a tremendous amount of event statistics in a given collision. In addition, the Hadron Forward (HF) calorimeters cover the region, $2.9 < \mid \eta \mid < 5.2$, providing forward event activity measurements crucial to E_T analyses such as Figure 1(right).

2.2 Solenoidal Tracker at RHIC (STAR)

The STAR detector was constructed to study strongly-interacting particles, such as the Upsilon meson, produced in ultrarelativistic collisions[13]. The goal of STAR is to understand hadron interactions at high energy densities and will thus provide the comparison needed to further interpret the high correlations observed at CMS. Charged particle identification is done via the Time Projection Chamber (TPC) in conjunction with the 0.5 T magnetic field. Since the STAR detector has such different systematics than CMS, similar physics results from each provides strong support for arguing that the observations are indeed valid physics rather than spurious detector effects.

Although construction of a Muon Telescope Detector(MTD) has recently reached completion [14], the data analyzed in this paper was reconstructed from 2012 p-p collisions in which Υ identification was done by the Barrel Electromagnetic Calorimeter(BEMC)[15]. Here a threshold of electron energy deposition of approx. 4.2 GeV was required in one of the towers (referred to as the "high tower"), along with an associated electron candidate patch on the opposite side of the detector(referred to as the "trigger patch"). Relevant quantities such as $n\sigma_e$ and the invariant mass of electron track-pairs are then recorded for further scrutiny.

3. Computational Methods

The polarization analysis to follow was constructed entirely in PYTHIA[16], with all plots generated using ROOT [17]. Parton distribution functions are taken from the MRSTMCal libraries under LHAPDF and relevant heavy-flavor customizations are employed to ensure all simulations emulate past experimental observations.

All polarization simulations are based off generating millions of proton-proton collisions, with the requirement that each event produces an Υ(1S) which then decays exclusively into a dimuon. All the relevant kinematic variables associated with the Υ(1S), μ^+, and μ^- are then stored in an ntuple to be used for further analysis. Using α as previously defined in (2), the Υ p_T is weighted by (2) and plotted for each polarization case: unpolarized(α = 0), transverse(α = 1), and longitudinal(α = -1). A pseudorapidity cut is then applied to each of the three datasets. For STAR the cut is $|\eta|$<1.0; For CMS the cut is $|\eta|$<2.4. The acceptance plots are then simply the ratio of the cut data subset over the initial dataset. Another similar process is done in which the initial dataset consists only of events in which the muons satisfied certain kinematic properties (to be discussed later). These plots will be referred to as the kinematic acceptance plots to distinguish them from the prior, uncut baseline.

4. Polarization Acceptance Plots

Before analyzing possible polarization effects at CMS, a simulation is made to emulate STAR to match results already published. These polarization acceptances for STAR are shown in Figure 2 [5]. They are presented here primarily to convince the reader of the validity of the plots to follow. Notable features of the superimposed acceptance include the crossover around 3 GeV/c and the monotonic increase in acceptance for higher p_T. The acceptance differences for low p_T are intuitive when one visualizes the Υ decay as seen by the lab frame. For example, if full transverse polarization is assumed(i.e. decay along Υ momentum axis), and the Υ has low p_T, the dimuon will have momentum primarily along the z-axis and will thus not be detected.

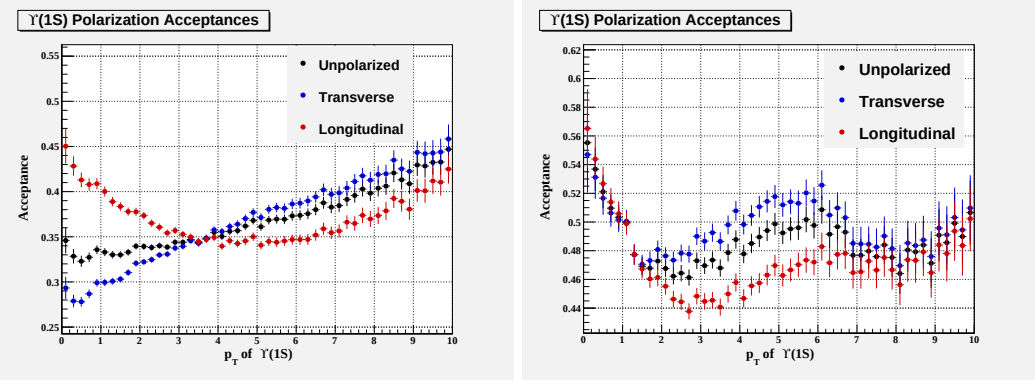

Figure 2: Acceptance yields for varying degrees of Υ(1S) polarization simulated at 200 GeV for the STAR detector. On the left, only a pseudorapidity cut of $|\eta| < 1.0$ is applied to the full dataset, with the ratio $\frac{N_{cut}}{N_{all}}$ defined as the acceptance. On the right, baseline cuts of $p_T^{(1)} < 4$ GeV/c, $p_T^{(2)} < 2.5$ GeV/c, and $cos(\theta) < 0.5$ are applied. From there, the same pseudorapidity cut $|\eta| < 1.0$ is applied, with the ratio $\frac{N_{\eta cut}}{N_{baseline}}$ defined as the acceptance.

[5] The plots indeed mirror those produced by STAR member Thomas Ullrich [5].

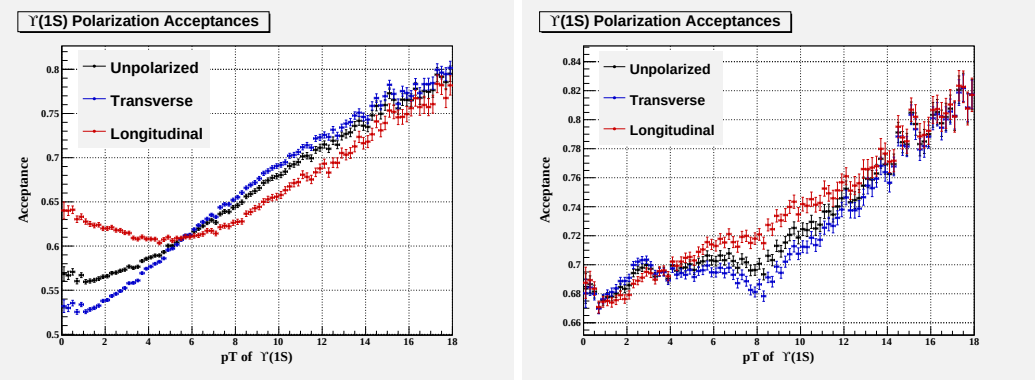

Figure 3: Acceptance yields for varying degrees of Υ(1S) polarization simulated at 2.76 TeV for the CMS detector. On the left, a pseudorapidity cut of $\mid \eta \mid < 2.4$ is applied to the full dataset, with the ratio $\frac{N_{cut}}{N_{all}}$ defined as the acceptance. On the right, baseline cuts of $p_T^{(1)} < 4$ GeV/c and $p_T^{(2)} < 3.5$ GeV/c are applied. From there, the same pseudorapidity cut $\mid \eta \mid < 2.4$ is applied, with the ratio $\frac{N_{\eta cut}}{N_{baseline}}$ defined as the acceptance.

The CMS analysis was then constructed by the processes introduced above in Section 3. Proton-proton collisions are run at $\sqrt{s} = 2.76TeV$ as is typically done at CMS, and the cut of $\mid \eta \mid < 2.4$ emulates the acceptance region of the muon detector system. The acceptances plots are shown above in Figure 3. The shapes of the acceptances are visually similar to those found for the STAR detector with expected differences. For example, the acceptance crossover in the left figure occurs at a higher value of Υ p_T and the absolute values of acceptance are higher. This can be explained by the higher range of acceptance allowed at CMS compared to STAR's acceptance of $\mid \eta \mid < 1.0$.

The kinematic acceptances indicate that the polarization systematic uncertainty is smaller at CMS than at STAR. The level of systematic uncertainty is estimated by the vertical distances between polarization cases in a given bin. The difference communicates how much the expected Υ yield may vary depending on the true degree of polarization. Since a p_T threshold is often set as a trigger for dimuon candidates detected in a collision, as was done for the simulated kinematic acceptances, this plot indicates how the true polarization may affect Υ yields for a typical CMS run.

The statistical errors are negligibly small due to the high number of events simulated and would decrease further with even more simulated collisions. They were calculated using a Bayesian approach, briefly outlined as follows: Consider a single bin with content k/n, where k is a subset of n total events that passed a certain efficiency cut. Rather than estimating the efficiency (denoted ξ)to be merely k/n, we use a probability distribution relating the probability that the true efficiency is ξ, *given* that k out of n events passed the cut [18],

$$P(\xi; k, n) = \frac{(n+1)!}{k!(n-k)!}\xi^k(1-\xi)^{n-k} \tag{3}$$

which has been derived from Bayes' theorem assuming a uniform prior for $P(\xi; n)$, so as not to favor any particular efficiency value. From this distribution we find the standard deviation:

$$\sigma = \sqrt{\frac{(k+1)}{(n+2)}\frac{(k+2)}{(n+3)} - \frac{(k+1)^2}{(n+2)^2}} \tag{4}$$

This was the quantity used to calculate the statistical error associated with each bin for the polarization acceptance plots[6]

[6]The full derivation may be found in Ref.[18].

The takeaway from these acceptances is a new intuition regarding how polarization affects Upsilon yields, or acceptances, at a particle detector like CMS. When extracting Upsilons from a raw dataset, a prior expectation of how many Upsilons one ought to observe is inevitably factored into the analysis, and could thus skew the results if polarization effects are not properly taken into account.

5. Yield Extraction and Event Activity at STAR

Motivated by the results from CMS, a 2012 proton-proton dataset from STAR (from section 2.2) is analyzed for any correlations between Υ(nS) yields and event activity. The central rapidity region's event activity will be measured by a value called reference multiplicity, defined as the number of charged particle tracks within a given pseudorapidity range. This analysis is primarily interested in comparing the Υ yields in given ranges of reference multiplicity as a means of comparison to the recent CMS measurements. Accordingly, the method of analysis will be to bin the multiplicity in two distinct rapidity bins, with one bin in the same acceptance region as the Upsilon and with the other in a slightly more forward/backward region.

First, the data with all Upsilon candidates is collected and preliminary cuts are applied. Guided by past results, the data is cut to only allow electrons satisfying the following [7]:

$$-1.2 < n\sigma_e < 3 \qquad \text{and} \qquad 0.7 < \frac{E_i}{p_i} < 1.3 \qquad \text{and} \qquad 8.0 < m_{e^+e^-} < 11$$

Using these cuts, the invariant mass of the dielectrons are plotted in a histogram in Figure 4(left). A color distinction is made between electron pairs of opposite charge (red) and of like charge (blue). Oppositely charged pairs are expected to have originated from an Upsilon, due to charge conservation (the Υ has zero charge). The like-charge electron pairs are considered to be background originating from processes such as $b - \bar{b}$ production and the Drell-Yan process[19].

To maximize the number of good Upsilon candidates from this dataset, we want to maximize a quantity called the effective signal, S_{eff}[20]:

$$S_{eff} = \frac{S}{2\frac{B}{S} + 1}$$

where [8]

$$S = \int_8^{11} (m_{unlikeCharge} - m_{likeCharge})dm \qquad \text{and} \qquad B = \int_8^{11} m_{likeCharge}dm$$

A maximized S_{eff} is associated with a maximized Υ yield extracted from the dataset. The primary method employed here was to scan different ranges of possible cuts to the data and, for each cut range, to find the value of S_{eff}. Once a maximum is found in this abstract cut space, those cuts are kept and applied to the dataset. Figure 4 (right) shows two examples of searched cut ranges for the quantities $n\sigma_e$ and $\frac{E_1}{p_1}$. In all these cut scans, the following global cut is applied to the data being scanned: $0.5 <\mid y \mid < 1.5$. In addition, S_{eff} is evaluated by integrating *outside* the Υ mass range defined in the integrals above. These restrictions are applied to ensure no artificial optimization is occurring so as to avoid possible autocorrelations. Upsilons are expected in the rapidity range $\mid y \mid < 0.5$ and that is the cut applied to all later fits. The maximized S_{eff} is simply used as a guide for which cuts ought to be applied to future fits.

[7] Any *i*'s just means the cut was applied to both electrons

[8] Henceforth, all variables denoted *m* are referring to the invariant mass of the electron-pair.

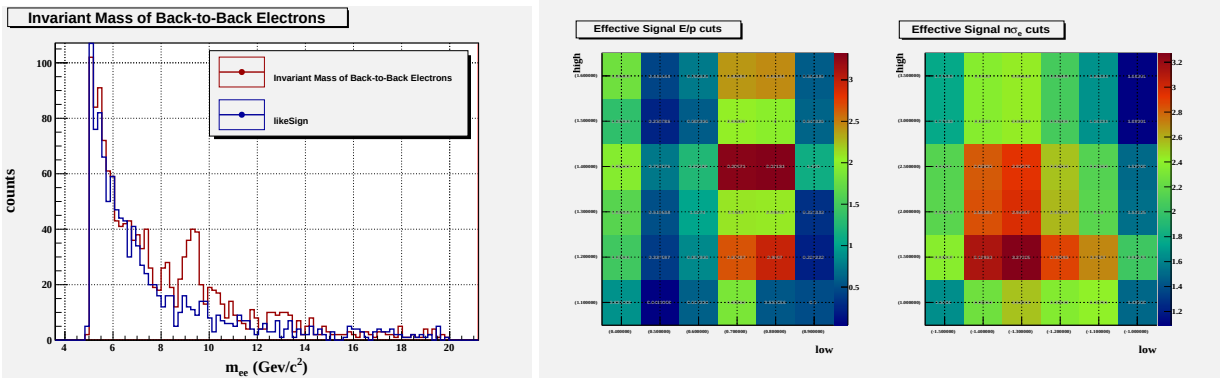

Figure 4: (left) Dielectron invariant mass distribution from 2012 STAR Υ(nS) candidate dataset. A clear peak can be seen at 9.46 GeV/c^2, the mass of the $\Upsilon(1S)$ meson. (right) Scanning the cut space for maximum S_{eff}. The leftmost scan is on electron $\frac{E}{p}$ cuts, where the rightmost scan is on $n\sigma_e$ cuts. The x-axis corresponds to a low-end value for a cut range, and the y-axis corresponds to the high-end value. Each plot scans a single variable cut range. Many plots are produced, each corresponding to different variables in order to observe how each variable affects the S_{eff}.

With a potential maximum S_{eff}, the invariant mass data with optimized cuts is plotted against a fitted Crystal-Ball function (Figure 5). From the fitted model, Υ(nS) yields are extracted with statistical errors taken into account. The data is integrated over all reference multiplicity, defined as the number of tracks found in the detector regions

$$0 < |\ \eta_{e^+e^-}\ | < 0.5 \text{ [refMult1]} \qquad \text{or} \qquad 0.5 < |\ \eta_{e^+e^-}\ | < 1.0 \text{ [refMult2]}$$

depending on which reference multiplicity is being analyzed. The former is the region closest to midrapidity (where the Upsilon is measured) and the latter is in a bin that is slightly more forward/backward. For compactness, only refMult1 is shown in Figure 5, whereas both are shown in Figure 6. Regardless of which reference multiplicity is used, an average of fifty-five Upsilons were found per event in the dataset.

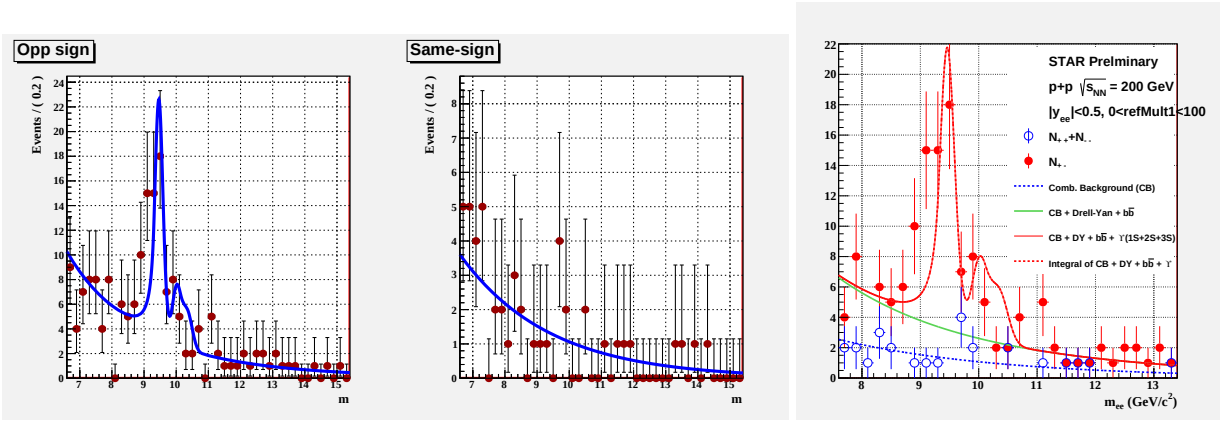

Figure 5: Invariant mass data fit to a CB function integrated over all values of reference multiplicity. From left to right, invariant mass is plotted for (1) unlike-charge electron pairs, (2) like-charge electron-pairs, and (3) for both, using a more sophisticated fitting macro. These fits were applied to the same cut dataset and they extracted an average of fifty-five Upsilons per event.

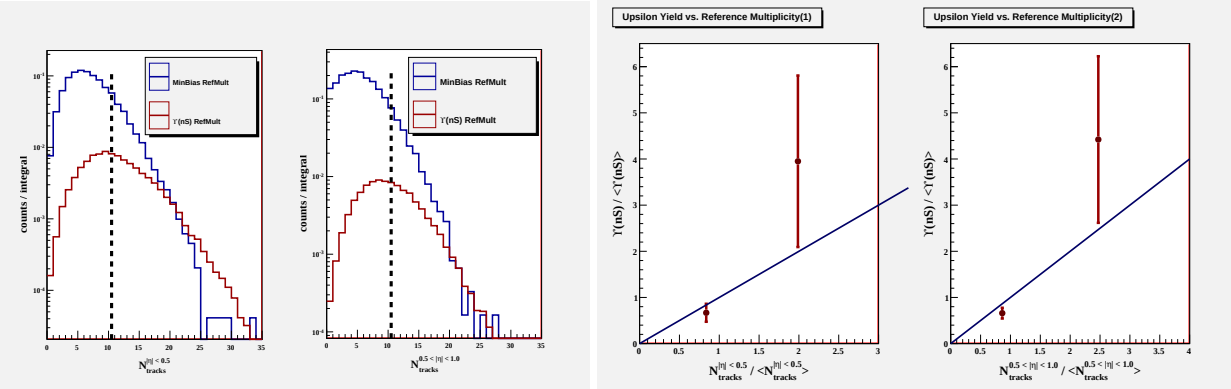

Figure 6: (left) Reference multiplicity distributions plotted for all events[blue] and a subset of these events with Υ candidates [red]. A vertical dashed line is drawn to illustrate where reference multiplicities were divided to produce the plot on the right. (right) Event-normalized Υ yields versus their event-normalized reference multiplicities (same axes as in Figure 1 (left). Lack of statistics is due to having only half of the data expected.

Now that the average number of Upsilons found in all events using optimized cuts has been found, this value will be used as the event average, $< \Upsilon(nS) >$, or activity-integrated value of Upsilons produced. The relationship of interest is whether or not the fractional Upsilon yield, $\frac{\Upsilon(nS)}{<\Upsilon(nS)>}$ (where the numerator is the average $\Upsilon(nS)$ yield for a given reference multiplicity range), exhibits a positive correlation when plotted against the event-normalized reference multiplicity, $\frac{refMult}{<refMult>}$. To plot these quantities, we need to split up the reference multiplicity distributions and extract the average $\Upsilon(nS)$ from each (Figure 6). The dataset extends out to a reference multiplicity of one-hundred, but the vast majority of events recorded a reference multiplicity value under twenty. To have a (somewhat) more even split, then, the data is cut into two sections corresponding to events with less than ten tracks found and events with more than ten tracks found. The average $\Upsilon(nS)$ yields found on either side of this cut are extracted and their event-normalized values are plotted as a function of the corresponding event-normalized reference multiplicity values (Figure 6(right)).

Interpretation of these plots is limited, due to the large statistical uncertainties and lack of data points. Using this dataset, more points would raise the statistical uncertainty, and less points would offer nothing for an analysis. Nonetheless, an undeniable positive correlation exists. What is uncertain is whether or not this correlation is linear (as was originally expected) or perhaps quadratic (as the CMS results appear to suggest). More data will be needed to confirm or deny the possibility of a nonlinear correlation.

6. Conclusions

The relative acceptances associated with the polarization of the Upsilon meson at CMS do not appear to differ drastically from the same acceptances simulated for STAR. The vertical distances between the three polarization cases indicates the associated systematic uncertainty. The absolute systematic errors for CMS are identical to those for STAR at low Υ p_T and no applied kinematic cuts. They differ, however, in the case of kinematic acceptances such that the systematic error is *lower* at CMS when compared to STAR. This suggests that polarization effects on detector acceptance may depend on the event energy.

The event activity results from STAR suggest a positive correlation between event-normalized Upsilon yields and the corresponding event-normalized reference multiplicities, albeit with too few statistics to provide for stronger conclusions. It should be noted that, when experimenting with different regions of reference multiplicity to extract from for Figure 6(left), the level of positive correlation varied both above and below the line with slope unity. Nonetheless, there is a clear (expected) positive correlation between $\Upsilon(nS)$ yields and central event activity.

7. Acknowledgements

The work presented here would not have been possible without all the help and support given by the National Science Foundation, Dr. Rena Zieve, and the Nuclear Physics Group at UC Davis. In particular, graduate students Chad Flores, Anthony Kesich, and Chris Flores have played direct roles in the above analyses and have greatly expanded my knowledge in the realm of high-energy physics. Professors Manuel Calderón and Daniel Cebra lead an excellent research group and deserve the highest commendation for their interest in undergraduate outreach. Professor Calderón in particular has introduced me to this field, guided me throughout every step of my research, and been a role model for the research scientist and person I'd like to become. I cannot express my gratitude enough for being given the opportunity to work with such fantastic individuals.

References

[1] T. Matsui and H. Satz, Phys. Lett. B **178**, 416 (1986).

[2] CMS Collaboration, "Observation of Sequential Υ Suppression in PbPb Collisions", *Phys. Rev. Lett.* **109**, 222301 (2012). DOI:10.1103/PhysRevLett.109.222301

[3] Phys. Lett. B 735 (2014) 127 10.1016/j.physletb.2014.06.028

[4] CMS Collaboration, "Measurement of the $\Upsilon(1S)$, $\Upsilon(2S)$, and $\Upsilon(3S)$ polarizations in pp collisions at $\sqrt{s}$ = 7 TeV", CMS-BPH-11-023 (2013).

[5] T. Ullrich, "Private Communication".

[6] D∅ Collaboration, "Measurement of the Polarization of the $\Upsilon(1S)$ and $\Upsilon(2S)$ States in $p\bar{p}$ Collisions at $\sqrt{s}$ = 1.96 TeV", *Phys. Rev. Lett.* **101**, 182004 (2008).

[7] CDF Collaboration, "Measurements of the Angular Distributions of Muons from Υ Decays in $p\bar{p}$ Collisions at $\sqrt{s}$ = 1.96 TeV", *Phys. Rev. Lett.* **108**, 151802 (2012).

[8] B. Gong, J.-X. Wang, and H.-F. Zhang, "QCD corrections to Υ production via color-octet states at the Tevatron and LHC", Phys. Rev. D **83** (2011) 114021, doi:10.1103/PhysRevD.83.114021.

[9] CMS Collaboration,"Event activity dependence of Υ(nS) production in $\sqrt{s_{NN}}$ = 5.02 TeV pPb and $\sqrt{s}$ = 2.76 TeV pp collisions", *JHEP04* (2014). doi:10.1007/JHEP04(2014)103.

[10] H. Abramowicz et al., "Summary of the workshop on multi-parton interactions (MPI@LHC 2012)", (2013). arXiv:1306.5413.

[11] P. Bartalini, E. Berger, B. Blok, et al., "Multi-Parton Interactions at the LHC", (2011). arXiv:1111.0469v2

[12] CMS Collaboration, "The CMS experiment at the CERN LHC", JINST (2008) S08004, doi:10.1088/1748-0221/3/08/S08004.

[13] STAR Collaboration, "STAR Detector Overview", *Nucl. Inst. and Meth. A* **499** (2003) 624-632.

[14] L. Ruan et al., "Perspectives of a Midrapidity Dimuon Program at RHIC: A Novel and Compact Muon Telescope Detector", (2009). arXiv:0904.3774v4

[15] STAR Collaboration, "Υ cross section in p + p collisions at $\sqrt{s}$ = 200 GeV", (2010). http://arxiv.org/abs/1001.2745v2

[16] *PYTHIA Homepage*, http://home.thep.lu.se/ torbjorn/Pythia.html

[17] *ROOT Homepage*, http://root.cern.ch/drupal/

[18] T. Ullrich, & Z. Xu, "Treatment of Errors in Efficiency Calculations", (2007). http://export.arxiv.org/abs/physics/0701199v1

[19] I. Kenyon, "The Drell-Yan Process", *Rep. Prog. Phys.* **45** (1982).

[20] T. Ullrich, "What is the Effective Signal and what is it good for?" (2009). http://phys.kent.edu/ margetis/STAR/D0/NoteOnEffSignal.pdf